The Journal of Chemical Physics

Thermodynamic analysis of the stability of planar interfaces between coexisting phases and its application to supercooled water

Cite as: J. Chem. Phys. **150**, 224503 (2019); https://doi.org/10.1063/1.5097591
Submitted: 26 March 2019 . Accepted: 09 May 2019 . Published Online: 10 June 2019

Rakesh S. Singh, Jeremy C. Palmer, Athanassios Z. Panagiotopoulos, and Pablo G. Debenedetti

The Journal of Chemical Physics ARTICLE scitation.org/journal/jcp

Thermodynamic analysis of the stability of planar interfaces between coexisting phases and its application to supercooled water

Cite as: J. Chem. Phys. 150, 224503 (2019); doi: 10.1063/1.5097591
Submitted: 26 March 2019 • Accepted: 9 May 2019 •
Published Online: 10 June 2019

Rakesh S. Singh,[1,a] Jeremy C. Palmer,[2] Athanassios Z. Panagiotopoulos,[1] and Pablo G. Debenedetti[1,b]

AFFILIATIONS

[1] Department of Chemical and Biological Engineering, Princeton University, Princeton, New Jersey 08544, USA
[2] Department of Chemical and Biomolecular Engineering, University of Houston, Houston, Texas 77204, USA

Note: This paper is part of a JCP Special Topic on Chemical Physics of Supercooled Water.
[a] **Current address:** Department of Chemistry, Indian Institute of Science Education and Research (IISER), Tirupati, Andhra Pradesh 517507, India.
[b] **Author to whom correspondence should be addressed:** pdebene@princeton.edu

ABSTRACT

Two-phase simulations are commonly used to evaluate coexistence conditions, interfacial tensions, and other thermodynamic properties associated with first-order phase transitions. Calculation of these properties is often simplified when the interfaces between the two phases are flat or planar. Here, we derive a general thermodynamic criterion for selecting simulation cell dimensions to stabilize planar interfaces in phase-separated fluid-fluid systems with respect to homogeneous, single-phase states. The resulting expression is validated by analyzing the effects of simulation cell dimensions on the formation of planar liquid-vapor interfaces in the Lennard-Jones fluid and in the TIP4P/2005 model of water. We also perform large scale molecular dynamics simulations to study metastable liquid-liquid phase separation in the ST2 and TIP4P/2005 models of water under deeply supercooled conditions. Our simulations confirm the stability of a liquid-liquid interface in ST2, and they demonstrate that the corresponding interface for TIP4P/2005 can be stabilized by judiciously choosing the simulation cell aspect ratio in a manner consistent with the thermodynamic criterion. We posit that this sensitivity to the simulation cell aspect ratio may explain discrepancies between previous studies examining liquid-liquid separation in models of supercooled water.

I. INTRODUCTION

Computational[1–12] and theoretical[13–18] studies of interfaces associated with first-order phase transitions have played an important role in helping to develop an improved understanding of finite-size effects[2,6,8,12,16] as well as in enabling the calculation of interfacial tensions, free energy barriers, and other thermodynamic quantities associated with such phase transitions.[1,3–5,7,9–11,19–21] Although most interface-explicit computational studies to date have focused on the liquid-vapor transition, the crystal-vapor (e.g., Ref. 22), crystal-solution (e.g., Ref. 23), and crystal-melt (e.g., Refs. 24–26) interfaces have also been investigated. Explicit simulation of interfaces is also of interest in biophysics and cell biology (e.g., Ref. 27), especially in light of the currently active area of intracellular liquid-liquid transitions and their possible role in the compartmentalization of important cell functions (e.g., Refs. 28 and 29).

Molecular simulations have been an essential tool in the investigation into the possibility that deeply supercooled water possesses a liquid-liquid transition terminating at a second, metastable critical point (e.g., Refs. 30–32). In fact, the very hypothesis of the existence of a liquid-liquid phase transition in water was formulated in a computational study.[33] Experimental (e.g., Refs. 34 and 35) and computational (see Ref. 32 for a recent review) studies of supercooled water and its possible transition between low- and high-density liquid (LDL and HDL) phases remain an active area of research[30] more than 40 years after Speedy and Angell first called the attention of the scientific community to the behavior of water's response functions and transport coefficients upon supercooling.[36]

The majority of computational studies of supercooled water addressing the possibility of a liquid-liquid transition have involved equation-of-state calculations or free energy studies.[32] Nevertheless, important work has also been performed involving direct simulation of interfaces. Yagasaki *et al.* reported spontaneous liquid-liquid phase separation (LLPS) and the formation of a stable interface in canonical molecular dynamics (MD) simulations of the ST2 model of water,[37] with reaction field treatment of long-range electrostatic forces (ST2-RF).[38] These authors isochorically quenched an initially homogeneous system consisting of 4000 water molecules from supercritical to estimated subcritical conditions and followed the time evolution of the resulting unstable system. Analogous conclusions were reached for the TIP4P/2005[39] and TIP5P[40] models. English *et al.* tested the mechanical stability of HDL–LDL interfaces in the ST2, TIP4P,[41] and SPC/E[42] models.[43] They used canonical MD simulations of inhomogeneous systems consisting of HDL and LDL regions separated by a flat interface, with an overall density close to the estimated critical density for each model, at subcritical temperatures. They observed rapid density equalization and concluded that the liquid-liquid transition does not exist because their HDL–LDL interface is mechanically unstable. However, the initial condition chosen by English *et al.* is far from equilibrium (the pressures in the HDL and LDL regions differed by as much as 5 kbar), and the subsequent behavior of the system is entirely consistent with expectations, and, contrary to the authors' claim, does not test the mechanical stability of an equilibrium HDL–LDL interface at coexistence.[32]

Overduin and Patey performed calculations analogous to those of Yagasaki *et al.*,[38] focusing on the TIP4P/2005 and TIP5P systems.[44] They found that the density of the subcritically quenched systems became progressively uniform upon increasing the sample size from 4000 to 32 000 water molecules, with no evidence of phase separation reported for $N = 32\,000$. Accordingly, Overduin and Patey concluded that the observations of Yagasaki *et al.* for TIP4P/2005 and TIP5P were a small-system artifact. Overduin and Patey also hypothesized that Yagasaki *et al.*'s observations for ST2 may also be the result of the (relatively) small system size used by these authors. Guo *et al.* recently tested the small-system-artifact hypothesis of Overduin and Patey.[45] They simulated 256 000 ST2-RF molecules and, upon quenching isochorically to subcritical conditions, they observed spontaneous phase separation and the formation of a stable planar interface between the HDL and LDL phases. Spontaneous liquid-liquid phase separation and the formation of a stable interface upon isochoric quenching into the coexistence region was also recently reported in large scale simulations (up to $N = 432\,000$) of an ionic model of silica, a tetrahedral system displaying waterlike anomalies.[46,47]

With an eye toward clarifying some of the above-summarized contrasting claims about the stability (or lack thereof) of the interface separating the low- and high-density phases of supercooled water, we derive a simple and general (i.e., not water-specific) thermodynamic criterion for the stability of a flat interface in simulations of first-order fluid-fluid phase transitions. The thermodynamic criterion takes the form of an inequality. If the geometry of the simulation cell is chosen so that the inequality is satisfied [e.g., by choosing $L_z \gg (L_x = L_y)$, where z is the direction normal to the interface and L_x, L_y, and L_z are the dimensions of the simulation cell], the phase-separated system is predicted to be stable with respect to the homogeneous state.

The rest of this paper is organized as follows. Section II details the computational protocols for our vapor-liquid and liquid-liquid simulations. The thermodynamic criterion for the stability of a planar interface is derived in Secs. III and IV includes numerical tests of its validity for the vapor-liquid transition of the Lennard-Jones (LJ) and TIP4P/2005 systems. In Sec. V, we confirm the stability of the HDL–LDL interface for ST2-RF, and we demonstrate that the corresponding interface for TIP4P/2005 is stabilized by modifying the aspect ratio of the simulation cell in a manner consistent with the thermodynamic inequality. We also provide numerical evidence of the stability of the HDL–LDL interface with respect to rapid crystallization. The major conclusions from this work are summarized in Sec. VI, where we also provide suggestions for future work.

II. SIMULATION PROTOCOL

A. Vapor-liquid phase separation

Canonical (NVT) ensemble MD simulations were performed to investigate vapor-liquid phase separation (VLPS) in the LJ fluid and the TIP4P/2005[39] water model. Simulations of the LJ system were conducted using LAMMPS.[48] The LJ pair potential was truncated and shifted at a radial cut-off distance of $r_{\text{cut}} = 2.5\sigma$, where σ is the diameter of the LJ particle. The equations of motion were integrated using the velocity-Verlet algorithm with a $0.005\tau_{\text{LJ}}$ ($\tau_{\text{LJ}} = \sigma\sqrt{m/\epsilon}$, where m is the mass of the LJ particle and ϵ is the depth of the potential well) time step, and a Nosé-Hoover thermostat[49,50] with a $0.5\tau_{\text{LJ}}$ time constant was applied to maintain the system's temperature. The reported reduced critical temperature (T_c^*) and density (ρ_c^*) for this variant of the LJ model are 1.085 and 0.317, respectively[51] (note that, for the LJ model, all quantities are reported in reduced units so that the reduced temperature is $T^* = k_{\text{B}}T/\epsilon$ and reduced density is $\rho^* = \rho\sigma^3$, where k_{B} is Boltzmann's constant and T and ρ are the temperature and density in real units, respectively). Accordingly, to study vapor-liquid separation, simulations of an $N = 864$ particle system were performed at $T^* = 0.92$, 0.96, 0.98, and 1.00 along the critical isochore $\bar{\rho}^* = \rho_c^*$. Each simulation was equilibrated for an initial period of 10^6 time steps, followed by a production phase of 5×10^6 time steps, during which statistics were collected.

Simulations of TIP4P/2005 water were performed with GROMACS 4.6.5[52] for an $N = 864$ molecule system using the protocols described by Vega and de Miguel.[20] The short-range LJ part of the potential was truncated at 1.3 nm, and a switching function was applied between 1.2 and 1.3 nm to ensure that the potential and force smoothly converged to zero at the cut-off distance. Coulombic interactions were truncated at 1.3 nm, and the particle mesh Ewald method (PME)[53] was used to compute long-range contributions to the electrostatics. Parameters for the Ewald summation were chosen to ensure a relative error of less than 10^{-5} in the calculated energy. Trajectories were propagated using a 2 fs time step and a Nosé-Hoover thermostat[49,50] with a 0.2 ps time constant. The SETTLE algorithm[54] was used to handle TIP4P/2005's rigid body constraints. The vapor-liquid critical point for TIP4P/2005 is located at $T_c \sim 640$ K and $\rho_c = 0.31$ g cm^{-3}.[55] Thus, we conducted simulations

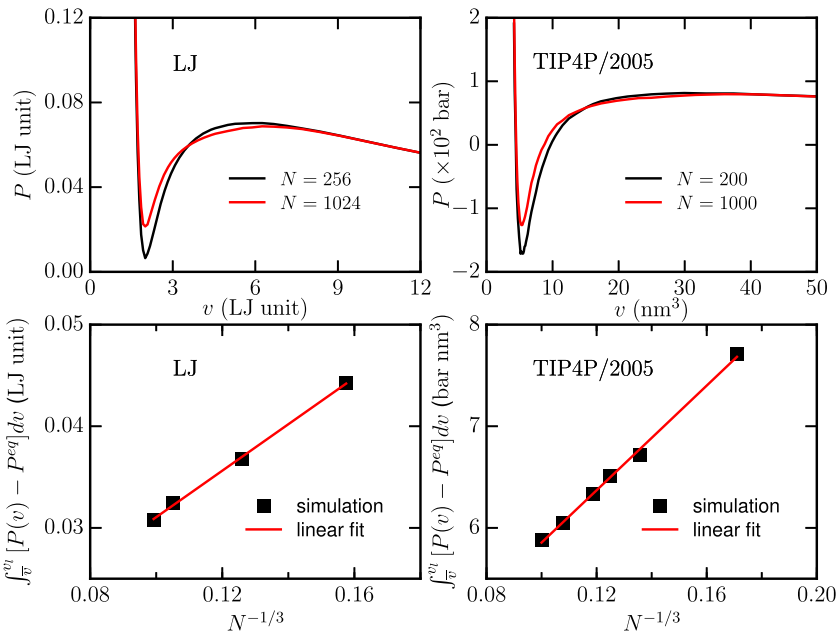

FIG. 1. The dependence of (top) VWL and (bottom) $\int_{\tilde{v}}^{v_l}[P(v) - P^{eq}]dv$ on system size (N) for the LJ model (left) and TIP4P/2005 (right). The simulations were performed at $T^* = 1.0$ ($T^*/T_c^* \sim 0.92$) and $\tilde{\rho}^* = 0.317$ for the LJ fluid and at $T = 580$ K ($T/T_c \sim 0.9$) and $\tilde{\rho} = 0.31$ g cm^{-3} for TIP4P/2005. The linear dependence of $\int_{\tilde{v}}^{v_l}[P(v) - P^{eq}]dv$ on $N^{-1/3}$ confirms Eq. (10).

at $T = 580$, 590, and 600 K along the $\tilde{\rho} = \rho_c$ isochore. The simulations were run for 10 ns, and properties were computed from the last 6 ns of each trajectory. For the MD simulations of TIP4P/2005 reported in Fig. 1, the cut-off distance for the short-range interactions was reduced to 0.9 nm to ensure consistency with the minimum image convention, and standard tail corrections were applied to the LJ interactions for both energy and pressure.

B. Liquid-liquid phase separation

Canonical ensemble MD simulations using GROMACS 4.6.5[52] were also performed to investigate LLPS in the TIP4P/2005 and ST2-RF water models. Details of our implementation of this ST2 variant are identical to those reported in Ref. 56. For TIP4P/2005, all short-range interactions were truncated at 0.95 nm and long-range electrostatics were treated using the PME method. Standard tail corrections were applied to the LJ interactions for both energy and pressure. The remaining simulation protocols follow those described in Sec. II A for TIP4P/2005. The reported liquid-liquid critical temperatures of ST2-RF and TIP4P/2005 are 247 K[56] and 182 K,[57,58] respectively. To avoid possible finite-size effects, the simulations of both models were conducted using large systems containing $N = 32\,000$ water molecules.

To observe the spontaneous LLPS, the model systems were first equilibrated at 300 K and then thermally quenched below their respective critical temperatures, into the two-phase region, to a final temperature T by instantaneously changing the set point of the thermostat. Simulations of ST2-RF were performed at $T = 236$ K ($0.96T_c$) and a fixed density of $\tilde{\rho} = 0.98$ g cm^{-3}, which is close to the estimated critical isochore.[56] Similarly, calculations for TIP4P/2005 were conducted at $T = 175$ K ($0.96T_c$) at the reported critical density $\tilde{\rho} = 1.02$ g cm^{-3}.[57] The characteristic relaxation times τ_{rlx} for ST2-RF and TIP4P/2005 under these conditions are ca. 30–40 ns (maximum observed hydrogen bond shuffle time in the LDL region of the composite system)[38] and ca. 50 ns (obtained from the stretched exponential fit of the composite system's self-intermediate scattering function at wavenumber $k = 18.6$ nm^{-1}),[44] respectively. Thus, to ensure equilibration, we performed long simulations varying between 300 and 400 ns for ST2 ($\sim 10 - 15\tau_{rlx}$) and 3–4 μs ($\sim 60 - 80\tau_{rlx}$) for TIP4P/2005. Properties such as liquid-liquid density profiles and the fraction of icelike molecules (Sec. V) were computed over the last ca. 150 ns and 1 μs of the trajectories for ST2 and TIP4P/2005, respectively.

III. THERMODYNAMIC CRITERION FOR A STABLE PLANAR INTERFACE

We consider coexisting fluid phases separated by a flat but, in general, finite-width interface. The system volume (V) can be expressed as

$$V = N\tilde{v} = N_l v_l + N_h v_h, \tag{1}$$

where N_l and N_h are the number of particles in the low-density (LD) and high-density (HD) phases, respectively, and $N = N_l + N_h$ is the total number of particles. $\tilde{v}$, v_l, and v_h are the mean specific volume of the overall system (V/N) and the corresponding quantities for the bulk coexisting LD and HD phases, respectively. As is customary in the Gibbs formulation of the thermodynamics of inhomogeneous systems, N_l and N_h correspond to the number of particles that would exist if the coexisting phases were homogeneous at their respective (bulk) coexisting densities, up to the Gibbs equimolar dividing surface. By definition, then, N_l and N_h add up to N, as written above. For VLPS, LD and HD correspond to the vapor and liquid phases (V and L), whereas LD and HD correspond to the LDL and HDL

phases in the context of LLPS. On defining the fraction of LD particles as $x = N_l/N$, Eq. (1) becomes

$$\bar{v} = xv_l + (1-x)v_h. \tag{2}$$

Solving for x, we obtain $x = (\bar{v} - v_h)/(v_l - v_h)$. The Helmholtz free energy of the above-defined phase-separated system (A_{PS}) can be expressed as

$$A_{PS} = A_l + A_h + \gamma F, \tag{3}$$

where A_l and A_h are the Helmholtz free energies of the bulk LD and HD phases and their homogeneous continuation up to the Gibbs equimolar dividing surface, γ is the surface tension (surface free energy per unit area), and F is the interfacial area between the coexisting phases. For spontaneous phase separation, with a stable interface between the coexisting phases, the free energy of the phase-separated system must be lower than the free energy of the finite-size system with no stable interface, $\bar{A}$,

$$A_l + A_h + \gamma F < \bar{A} \tag{4}$$

or,

$$N_l a_l + N_h a_h + \gamma F < N\bar{a}, \tag{5}$$

where a_k ($k = l, h$) denote the Helmholtz free energy per particle of the bulk LD and HD phases, and $\bar{a}$ is the Helmholtz free energy per particle of the finite-size system with no stable interface. The state that we have been describing as "finite-size system with no stable interface" would correspond, in the van der Waals picture, to a homogeneous unstable system.

Equation (5) can be rewritten in terms of the fraction of LD particles, x,

$$\gamma\frac{F}{N} < (a_l - a_h)(1-x) + (\bar{a} - a_l). \tag{6}$$

Using thermodynamic relations, $(a_l - a_h) = -P^{eq}(v_l - v_h)$ and $(\bar{a} - a_l) = -\int_{v_l}^{\bar{v}} P(v)dv$, we obtain

$$\gamma\frac{F}{N} < P^{eq}(\bar{v} - v_l) - \int_{v_l}^{\bar{v}} P(v)dv, \tag{7}$$

where P^{eq} is the coexistence pressure. The integral represents the finite-size estimate of the difference in specific Helmholtz free energies between the unstable and low-density states, calculated along the metastable and unstable portions of the isotherm (van der Waals loop, VWL). We use the fact that small-system simulations will naturally generate such a loop (see below). We furthermore derive a scaling relationship for this integral (Sec. IV), which we verify numerically and which allows extrapolation to other system sizes. We thus obtain the inequality

$$F < \frac{N\left[\int_{\bar{v}}^{v_l}(P(v) - P^{eq})dv\right]}{\gamma}. \tag{8}$$

For a planar interface, $N = \bar{\rho}FL_z$ or $F = N/\bar{\rho}L_z$ ($\bar{\rho} = 1/\bar{v}$ is the average number density of the system, and L_z is the simulation box length in the direction perpendicular to the interface), the above equation becomes

$$L_z > \frac{\gamma\bar{v}}{\left[\int_{\bar{v}}^{v_l}(P(v) - P^{eq})dv\right]}. \tag{9}$$

To observe spontaneous phase separation and the formation of a planar interface for a given system size N and temperature, Eqs. (8) and (9) suggest that the area of the planar interface must be lower than a critical interfacial area F^c defined by the right-hand side of Eq. (8). Accordingly, the elongated dimension of the rectangular simulation box must be larger than a critical length L_z^c defined by

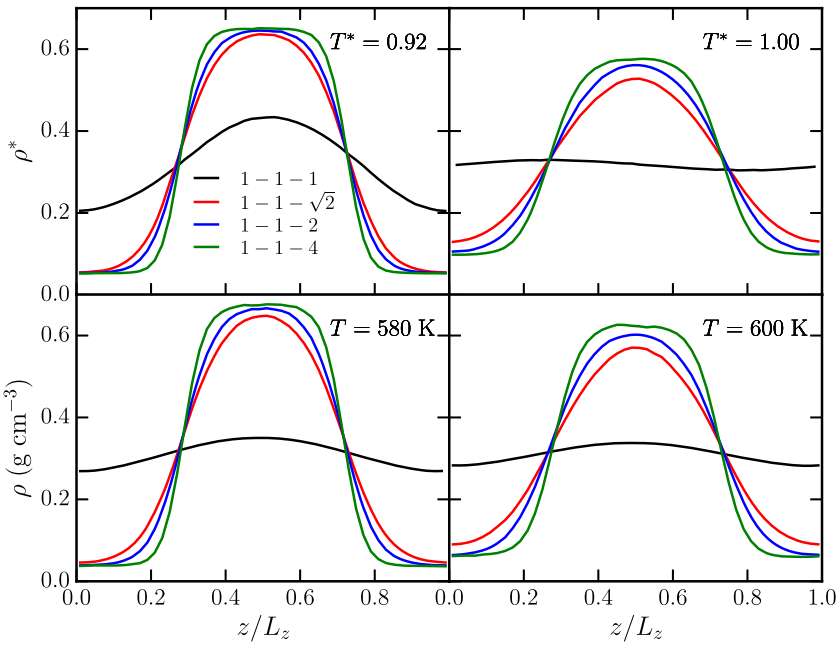

FIG. 2. Density profiles calculated for systems of $N = 864$ molecules using different simulation box aspect ratios for (top row) the LJ model and (bottom row) TIP4P/2005. The simulated temperatures are indicated in the legend of each panel. The system densities were fixed at $\bar{\rho}^* = 0.317$ and $\bar{\rho} = 0.31$ g cm^{-3} for the LJ model and TIP4P/2005, respectively.

the right-hand side of Eq. (9). The critical length of the simulation box depends on $\tilde{\rho}$, γ, and the VWL integral. The latter two quantities depend strongly on temperature and decrease as T increases toward the critical temperature.

The thermodynamic stability criterion in Eq. (9) is derived for the case where the coexisting phases are separated by a single planar interface. When simulations are performed with periodic boundary conditions, however, coexisting phases are separated by two planar interfaces (e.g., see Fig. 2). Consequently, the surface free energy contribution is twice as large and γ must be replaced by 2γ in Eqs. (8) and (9). Additionally, we note that even though the free energy of the phase-separated state is lower than the "unstable" (in the aforementioned, van der Waals sense) state [Eq. (4)], there is a possibility that a well-defined interface may not be observed in the close vicinity of a critical point. As T_c is approached from below, the interfacial energy $\gamma F/N$ becomes comparable to the thermal energy ($k_B T$) and interface formation is disrupted by thermal fluctuations. Hence, the underlying assumption in deriving Eqs. (8) and (9) is that the system temperature is sufficiently below T_c such that the interfaces are not smeared out by thermal fluctuations (i.e., $\gamma F/N \gg k_B T$).

We point out that Eq. (8), with an equal sign, can, in principle, be used to evaluate γ. Such thermodynamic integration approaches to the calculation of interfacial free energies are reviewed, e.g., in Refs. 59 and 60.

IV. SCALING BEHAVIOR OF THE VAN DER WAALS INTEGRAL AND NUMERICAL TEST OF EQ. (9)

Dimensional analysis of Eqs. (8) and (9), under the assumption that γ is independent of N, suggests the following scaling relation:

$$\int_{\tilde{v}}^{v_l} [P(v) - P^{eq}] dv \propto N^{-1/3}. \tag{10}$$

We have validated this prediction for the vapor-liquid transition in the LJ model and TIP4P/2005. $P(v)$ data from MD simulations of these models in a cubic cell were used to estimate P^{eq}, v_h, and v_l (via Maxwell's construction) and to evaluate the integral in Eq. (10) numerically. To accurately compute the integral in Eq. (10), $P(v)$ must be carefully equilibrated at each value of v to ensure proper sampling of fluctuations and inhomogeneities inside the coexistence region. The linear dependence of $\int_{\tilde{v}}^{v_l} [P(v) - P^{eq}] dv$ on $N^{-1/3}$ for both model systems confirms the scaling relation given by Eq. (10) (Fig. 1).

Equations (8) and (9) have also been validated numerically for the vapor-liquid transitions in the LJ model and in TIP4P/2005. The validation tests were conducted by first estimating the critical planar interfacial area F^c and box length L_z^c from Eqs. (8) and (9) using simulation data. These predictions were subsequently tested by monitoring for the formation of planar interfaces in direct phase coexistence simulations. Several factors were considered in selecting the system size and temperatures for these tests: (i) spontaneous phase separation will occur even in cubic boxes for large enough N or low enough T, frustrating accurate calculation of the VWL and hence F^c and L_z^c; (ii) the system must be large enough to accommodate the chosen potential cut-off distance; (iii) near T_c interfaces are diffuse, making it difficult to determine if phase separation has occurred. Using N = 864 molecules, however, we were able to identify suitable ranges of T for the LJ model and TIP4P/2005 (Table I). F^c and L_z^c were estimated from Eqs. (8) and (9) by numerically integrating $\int_{\tilde{v}}^{v_l} [P(v) - P^{eq}] dv$ as was done to validate Eq. (10). To ensure that the planar interfaces are well-separated and are not interacting with each other, the optimal choice for $\tilde{v}$ should be a value close to the critical mean specific volume, v_c (in reduced units, $v_c^* = 1/\rho_c^*$). For the LJ system, γ was calculated using grand canonical transition matrix Monte Carlo (GC-TMMC) simulations[61–64] (see the supplementary material). For TIP4P/2005, γ was estimated using a scaling relation parameterized by Vega and de Miguel.[20] Because tail corrections for LJ interactions were not included in our simulations of TIP4P/2005, these contributions were removed by subtracting extrapolated values from Table IV in Ref. 20 from the estimates of γ obtained from the scaling relation (see the supplementary material). The weak temperature dependence of F^c and L_z^c (Table I) results from the fact that the numerator and denominator terms in Eqs. (8) and (9) vary similarly with T and vanish as $T \to T_c$.

TABLE I. Theoretical estimates of the critical elongated box length L_z^c [Eq. (9)] and interfacial area F^c [Eq. (8)] for stability of a planar liquid-vapor interface in systems of N = 864 molecules. Predictions for the LJ model ($T_c^* = 1.085$) and TIP4P/2005 (T_c = 640 K) are for densities of $\tilde{\rho}^* = 0.317$ and $\tilde{\rho} = 0.31$ g cm^{-3}, respectively.

LJ			TIP4P/2005		
T^*	L_z^c (σ)	F^c (σ^2)	T(K)	L_z^c (Å)	F^c (Å^2)
0.92	14.1	193.3	580	45.3	1840.7
0.96	14.6	186.7	590	46.5	1792.6
0.98	15.0	181.6	600	48.8	1708.4
1.00	15.7	173.6	...	...	...

Direct phase coexistence simulations were performed to verify the predicted values of F^c and L_z^c. For each model, we considered four simulation cell aspect ratios and two different temperatures (Table II; Fig. 2). The formation of planar interfaces was monitored by computing the density profile along the elongated axis (z-axis) of the cell (Fig. 2). Drift in the location of the planar interface was accounted for by recentering the system's center of mass for each analyzed configuration. In both models, the formation of stable, planar vapor-liquid interfaces is observed in rectangular simulation boxes with aspect ratios $\geq \sqrt{2}$ (Fig. 2), in excellent agreement with the predictions of Eqs. (8) and (9) (Table I).

TABLE II. Aspect ratio dependent elongated box dimension (L_z) and the interfacial area perpendicular to the elongated box dimension (F) for systems of N = 864 molecules. The values reported for the LJ model and TIP4P/2005 are for densities of $\tilde{\rho}^* = 0.317$ and $\tilde{\rho} = 0.31$ g cm^{-3}, respectively.

Aspect ratio	LJ		TIP4P/2005	
($L_x - L_y - L_z$)	L_z (σ)	F (σ^2)	L_z (Å)	F (Å^2)
1-1-1	14.0	195.1	43.7	1908.5
$1-1-\sqrt{2}$	17.6	154.9	55.1	1514.8
1-1-2	22.2	122.9	69.3	1202.3
1-1-4	35.2	77.4	110.1	757.4

Because the morphology of the interface between the coexisting phases changes with the simulation cell aspect ratio, the shape of $P(v)$ and the integral $\int_{\tilde{v}}^{v_l}[P(v) - P^{eq}]dv$ in the two-phase region are expected to depend on the aspect ratio. In this work, however, we have not explored the sensitivity of this integral, and in turn, of F^c and L_z^c [Eqs. (8) and (9)], on the simulation cell aspect ratio used to evaluate $\int_{\tilde{v}}^{v_l}[P(v) - P^{eq}]dv$. This would be an interesting avenue for future inquiry.

V. STABILITY OF THE HDL–LDL INTERFACE: ASPECT RATIO DEPENDENCE

The main goal of this work is to investigate the stability of the HDL–LDL interface in the ST2-RF and TIP4P/2005 models. To this end, we study the effect of the simulation cell's aspect ratio on the density profiles at subcritical temperatures (Fig. 3). Due to the absence of available surface tension data and the computational cost associated with performing van der Waals integrations requiring numerous simulations spanning a range of densities at these low temperatures, we have not estimated F^c and L_z^c directly. Nonetheless, by increasing the cell aspect ratio, we are able to observe the formation of stable planar HDL–LDL interfaces in both water models (Fig. 3). Whereas LLPS in ST2-RF can be detected in each cell geometry examined (albeit with progressive sharpness as the box is made more elongated), the very possibility of observing an interface in TIP4P/2005 is sensitive to the cell aspect ratio. In accord with previous studies of TIP4P/2005,[44] we find no evidence of HDL–LDL phase separation in a system with N = 32 000 molecules when the

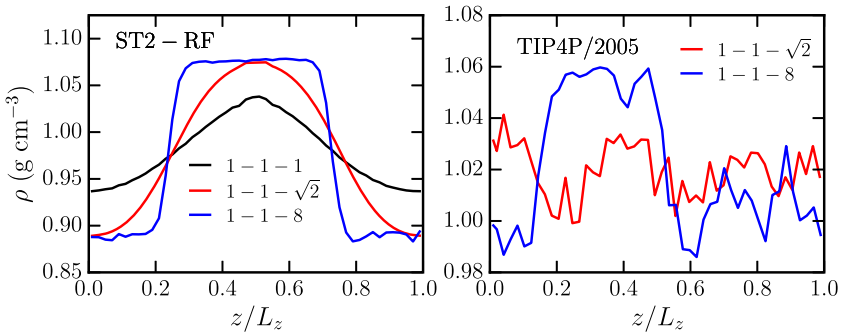

FIG. 3. Density profiles calculated for systems of N = 32 000 water molecules using different simulation box aspect ratios for (left) ST2-RF at T = 237 K and $\tilde{\rho}$ = 0.98 g cm^{-3} and for (right) TIP4P/2005 at T = 175 K and $\tilde{\rho}$ = 1.02 g cm^{-3}.

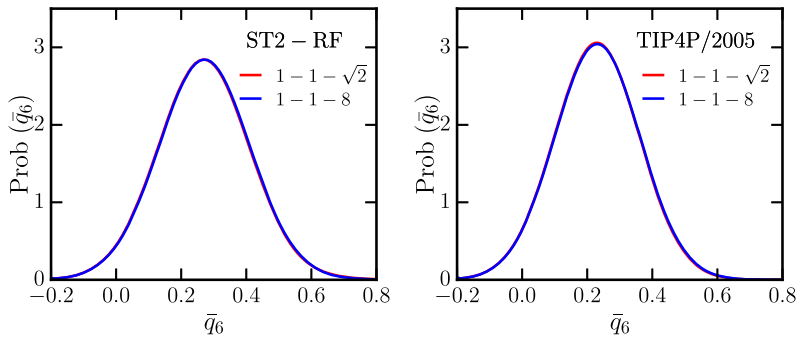

FIG. 4. Probability density distributions of the local order parameter $\bar{q}_6$ for (left) ST2-RF and (right) TIP4P/2005 for systems of N = 32 000 molecules at the same conditions reported in Fig. 3.

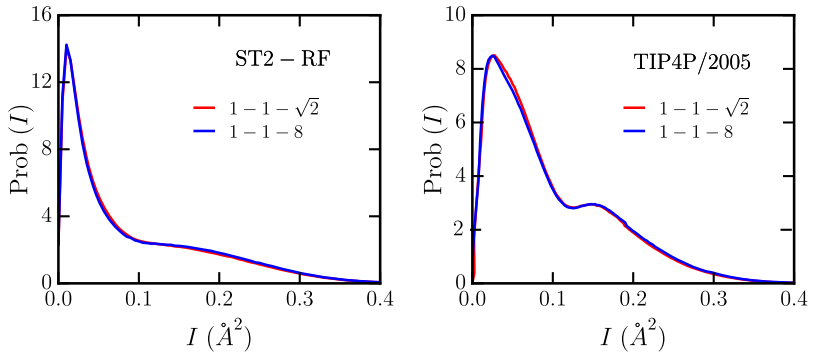

FIG. 5. Probability density distributions of the local structure index (I) for (left) ST2-RF and (right) TIP4P/2005 for systems of N = 32 000 molecules at the same conditions reported in Fig. 3.

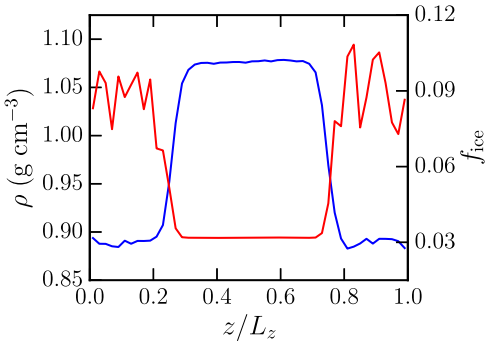

FIG. 6. Density (ρ) and fraction of icelike molecules ($f_{\rm ice}$) profiles (blue and red lines, respectively) for a N = 32 000 molecule system of ST2-RF in a simulation cell with a 1-1-8 aspect ratio. The thermodynamic conditions are the same as those reported in Fig. 3.

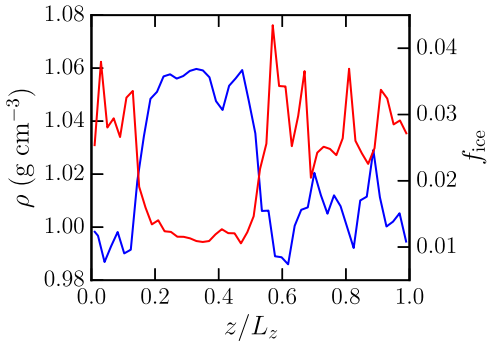

FIG. 7. Density (ρ) and fraction of icelike molecules ($f_{\rm ice}$) profiles (blue and red lines, respectively) for a N = 32 000 molecule system of TIP4P/2005 in a simulation cell with a 1-1-8 aspect ratio. The thermodynamic conditions are the same as those reported in Fig. 3.

cell aspect ratio is $1-1-\sqrt{2}$. Upon increasing the aspect ratio to 1-1-8, however, we observe planar HDL–LDL interfaces, similar to those reported in previous simulations for small systems with $N = 4000$ molecules.[38,44] This observation is consistent with the theoretical arguments outlined in Sec. III, which show that the use of a rectangular simulation cell may not be sufficient to stabilize planar interfaces between coexisting phases; one must choose the cell dimensions carefully to ensure that Eqs. (8) and (9) are satisfied for a given N and T.

To confirm that changing the cell aspect ratio does not fundamentally alter the structural properties of the system, we examined the distributions of the local bond-order parameter $\tilde{q}_6$ (Fig. 4)[65–67] and the local structure index (LSI) I (Fig. 5).[68] The parameter $\tilde{q}_6$ distinguishes between amorphous and crystalline local coordination environments,[69,70] whereas the LSI readily distinguishes between molecules with HDL-, LDL-, and icelike local order.[71] The presence of the latter is unavoidable in deeply supercooled liquids, which are expected to contain small subcritical ice nuclei. We observe that the distributions of both order parameters are insensitive to changes in the box aspect ratio. At the thermodynamic conditions studied here, the fraction of icelike molecules (i.e., molecules with $\tilde{q}_6 > 0.5$[70]) in ST2-RF and TIP4P/2005 is less than 6% and 3%, respectively. In both models, these values increase negligibly (<0.2%) upon changing the box aspect ratio from $1-1-\sqrt{2}$ to 1-1-8, consistent with the absence of significant differences between $\tilde{q}_6$ distributions computed for the two cell geometries (Fig. 4).

The spatial distribution of icelike molecules was analyzed by computing the profile $f_{\rm ice}(z) = n_{\rm ice}(z)/n_{\rm tot}(z)$, where $n_{\rm ice}$ and $n_{\rm tot}$ are the number of icelike molecules and total number of molecules, respectively, in a slab of width $dz \approx 0.8$ nm along the z-axis (major axis) of the simulation cell. The profile $f_{\rm ice}(z)$ for ST2-RF reveals that icelike molecules are preferentially found in the LDL region (Fig. 6). A similar result is also found for TIP4P/2005 (Fig. 7). This observation is consistent with studies showing that LDLlike domains, which are characterized by high local tetrahedral order and low mobility, serve as favorable locations for ice nucleation in deeply supercooled water.[72–76] Hence, these results imply that changing the simulation cell's aspect ratio to stabilize an interface alters the average spatial distribution of molecules instantaneously classified as HDL, LDL, and "icelike" according to an appropriate order parameter, but it does not appreciably influence their relative populations.

Finally, to ensure that crystallization is not interfering with the LLPS process, we examined the size of the largest icelike crystallite $n_{\rm ice}^{\rm largest}$ as a function of time (Fig. 8). A nearest-neighbor cutoff distance of 0.35 nm was applied to identify icelike molecules belonging to the same crystalline cluster. The absence of any noticeable increase in $n_{\rm ice}^{\rm largest}$ on the time scale relevant to the LLPS ($\tau_{\rm llps}$)

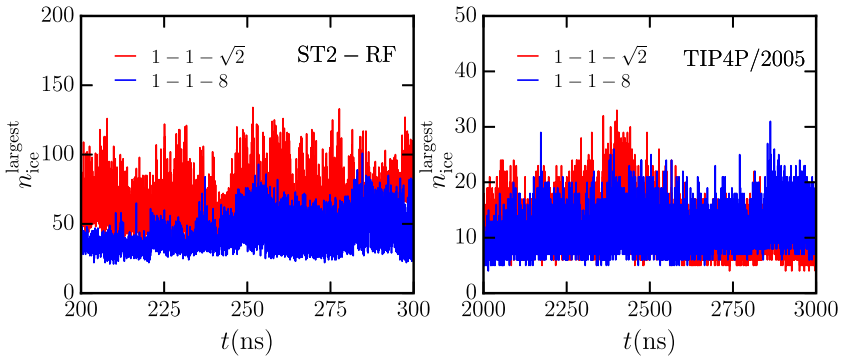

FIG. 8. The size of the largest icelike crystallite ($n_{\rm ice}^{\rm largest}$) as a function of time for (left) ST2-RF and (right) TIP4P/2005 after 200 ns and 2 μs of the initial relaxation, respectively, for the same systems and conditions reported in Fig. 3. The trajectory for ST2-RF and box aspect ratio $1-1-\sqrt{2}$ undergoes crystallization after >350 ns (not shown), which is more than an order of magnitude longer than the relaxation time $\tau_{\rm rlx} \approx 30$ ns;[38] no signs of crystallization were observed in the other simulations.

for both the models demonstrates that the characteristic crystallization time (τ_{cryst}) is significantly larger than τ_{llps} and τ_{rlx}, indicating that the coexisting metastable liquid phases can be fully equilibrated without interference from crystallization.

VI. CONCLUSIONS

In an effort to clarify conflicting claims regarding the stability of the HDL–LDL interface in previous computational studies,[38,43–46] we derived a simple and general inequality linking the minimum aspect ratio of a simulation cell needed to stabilize a flat interface between two coexisting fluid phases, as a function of system's physical properties [interfacial tension, mean density, free energy difference between the unstable (in the van der Waals sense) and one of the coexisting phases]. This simple relationship was derived by comparing the free energies of the finite-size system with no stable interface and the phase-separated stable (or metastable) system, the latter containing a flat interface. We tested the inequality numerically for vapor-liquid coexistence in the LJ and TIP4P/2005 systems and found that it accurately predicts the minimum elongation of the simulation cell required to observe a stable interface. We also verified a scaling prediction for the size-dependent $P(v)dv$ integral along metastable and unstable portions of the van der Waals loop generated in finite-size systems. This scaling behavior allows the calculation of this integral, required for the evaluation of the minimum aspect ratio needed to stabilize a flat interface, for systems of a few thousand molecules, based on $N \leq 1000$ calculations.

We next demonstrated that the HDL–LDL interface is stabilized by adequate choice of the aspect ratio (rectangular elongation) of the simulation cell, for both the ST2-RF and TIP4P/2005 systems. In particular, a simulation cell with an aspect ratio 1-1-8 clearly allowed the HDL–LDL interface to form and persist for times far in excess of the structural relaxation time. This result helps explain the origin of previous claims about the instability of the HDL–LDL interface.[38,43–46] We also showed that the metastable (with respect to crystallization) interface between the two coexisting liquids is well-defined thermodynamically since crystallization times significantly exceed the relevant liquid-phase relaxation times.[38,45]

In our investigation of the HDL–LDL interface, the inequality derived in Sec. III was used only qualitatively: the numerical calculation of the physical properties required for its quantitative application requires the deployment of computational resources even more significant than the ones used in this study. The accurate calculation of HDL–LDL interfacial tensions for molecular models of water over a range of temperatures, the equation of state calculations for a range of system sizes, such as to allow the numerical testing of the $N^{-1/3}$ scaling derived in this work for the van der Waals $P(v)dv$ integral, and extension of the present approach to the case of nonplanar interfaces are interesting avenues of future inquiry.

SUPPLEMENTARY MATERIAL

See supplementary material for the details of the calculation of vapor-liquid surface tension for the LJ fluid and the TIP4P/2005 water model.

ACKNOWLEDGMENTS

R.S.S. thanks Dr. Antonia Statt and Dr. Amir Haji-Akbari for helpful discussions. J.C.P. acknowledges support from the Welch Foundation (Grant No. E-1882). A.Z.P. acknowledges support by the Office of Basic Energy Sciences, U.S. Department of Energy, under Award No. DE-SC0002128. This work was conducted in part within the Computational Chemical Science Center: Chemistry in Solution and at Interfaces, which is funded by the U.S. Department of Energy under Award No. DE-SC0019394. Computations were performed at the Terascale Infrastructure for Groundbreaking Research in Engineering and Science (TIGRESS) at Princeton University and the Center for Advanced Computing and Data Systems at the University of Houston.

REFERENCES

[1] M. Rao and B. J. Berne, Mol. Phys. **37**, 455 (1979).
[2] D. J. Lee, M. M. Telo da Gama, and K. E. Gubbins, J. Chem. Phys. **85**, 490 (1986).
[3] M. J. P. Nijmeijer, A. F. Bakker, C. Bruin, and J. H. Sikkenk, J. Chem. Phys. **89**, 3789 (1988).
[4] M. Mecke, J. Winkelmann, and J. Fischer, J. Chem. Phys. **107**, 9264 (1997).
[5] A. Trokhymchuka and J. Alejandre, J. Chem. Phys. **111**, 8510 (1999).
[6] L. G. MacDowell, P. Virnau, M. Müller, and K. Binder, J. Chem. Phys. **120**, 5293 (2004).
[7] J. Vrabec, G. K. Kedia, G. Fuchs, and H. Hasse, Mol. Phys. **104**, 1509 (2006).
[8] L. G. MacDowell, V. K. Shen, and J. R. Errington, J. Chem. Phys. **125**, 034705 (2006).
[9] M. Schrader, P. Virnau, and K. Binder, Phys. Rev. E **79**, 061104 (2009).
[10] G. V. Lau, I. J. Ford, P. A. Hunt, E. A. Müller, and G. Jackson, J. Chem. Phys. **142**, 114701 (2015).
[11] C. Braga, J. Muscatello, G. Lau, E. A. Müller, and G. Jackson, J. Chem. Phys. **144**, 044703 (2016).
[12] A. Tröster, F. Schmitz, P. Virnau, and K. Binder, J. Phys. Chem. B **122**, 3407 (2018).
[13] J. G. Kirkwood and F. P. Buff, J. Chem. Phys. **17**, 338 (1949).
[14] T. L. Hill, J. Phys. Chem. **56**, 526 (1952).
[15] J. E. Mayer and W. W. Wood, J. Chem. Phys. **42**, 4268 (1965).
[16] K. Binder and M. H. Kalos, J. Stat. Phys. **22**, 363 (1980).
[17] A. J. Yang, J. Chem. Phys. **79**, 6289 (1983).
[18] A. J. Yang, J. Chem. Phys. **82**, 2082 (1985).
[19] R. S. Taylor, L. X. Dang, and B. C. Garrett, J. Phys. Chem. **100**, 11720 (1996).
[20] C. Vega and E. de Miguel, J. Chem. Phys. **126**, 154707 (2007).
[21] U. R. Pedersen, J. Chem. Phys. **139**, 104102 (2013).
[22] P. Koß, A. Statt, P. Virnau, and K. Binder, Mol. Phys. **116**, 2977 (2018).
[23] J. R. Espinosa, J. M. Young, H. Jiang, D. Gupta, C. Vega, E. Sanz, P. G. Debenedetti, and A. Z. Panagiotopoulos, J. Chem. Phys. **145**, 154111 (2016).
[24] J. R. Espinosa, E. Sanz, C. Valeriani, and C. Vega, J. Chem. Phys. **139**, 144502 (2013).
[25] J. R. Espinosa, C. Vega, C. Valeriani, and E. Sanz, J. Chem. Phys. **144**, 034501 (2016).
[26] A. Zaragoza, M. M. Conde, J. R. Espinosa, C. Valeriani, C. Vega, and E. Sanz, J. Chem. Phys. **143**, 134504 (2015).
[27] G. L. Dignon, W. Zheng, R. B. Best, Y. C. Kim, and J. Mittal, Proc. Natl. Acad. Sci. U. S. A. **115**, 9929 (2018).
[28] A. A. Hyman, C. A. Weber, and F. Julicher, Annu. Rev. Cell Dev. Biol. **30**, 39 (2014).
[29] Y. Shin and C. P. Brangwynne, Science **357**, eaaf4382 (2017).
[30] P. Gallo, K. Amann-Winkel, C. A. Angell, M. A. Anisimov, F. Caupin, C. Chakravarty, E. Lascaris, T. Loerting, A. Z. Panagiotopoulos, J. Russo *et al.*, Chem. Rev. **116**, 7463 (2016).

[31] N. J. Hestand and J. L. Skinner, J. Chem. Phys. **149**, 140901 (2018).
[32] J. C. Palmer, P. H. Poole, F. Sciortino, and P. G. Debenedetti, Chem. Rev. **118**, 9129 (2018).
[33] P. H. Poole, F. Sciortino, U. Essmann, and H. E. Stanley, Nature **360**, 324 (1992).
[34] J. Sellberg, C. Huang, T. McQueen, N. Loh, H. Laksmono, D. Schlesinger, R. Sierra, D. Nordlund, C. Hampton, D. Starodub *et al.*, Nature **510**, 381 (2014).
[35] K. H. Kim, A. Späh, H. Pathak, F. Perakis, D. Mariedahl, K. Amann-Winkel, J. A. Sellberg, J. H. Lee, S. Kim, J. Park *et al.*, Science **358**, 1589 (2017).
[36] R. J. Speedy and C. A. Angell, J. Chem. Phys. **65**, 851 (1976).
[37] F. H. Stillinger and A. Rahman, J. Chem. Phys. **60**, 1545 (1974).
[38] T. Yagasaki, M. Matsumoto, and H. Tanaka, Phys. Rev. E **89**, 020301 (2014).
[39] J. L. F. Abascal and C. Vega, J. Chem. Phys. **123**, 234505 (2005).
[40] M. W. Mahoney and W. L. Jorgensen, J. Chem. Phys. **112**, 8910 (2000).
[41] W. L. Jorgensen, J. Chandrasekhar, J. D. Madura, R. W. Impey, and M. L. Klein, J. Chem. Phys. **79**, 926 (1983).
[42] H. J. C. Berendsen, J. R. Grigera, and T. P. Straatsma, J. Phys. Chem. **91**, 6269 (1987).
[43] N. J. English, P. G. Kusalik, and J. S. Tse, J. Chem. Phys. **139**, 084508 (2013).
[44] S. D. Overduin and G. N. Patey, J. Chem. Phys. **143**, 094504 (2015).
[45] J. Guo, R. S. Singh, and J. C. Palmer, Mol. Phys. **116**, 1953 (2018).
[46] R. Chen, E. Lascaris, and J. C. Palmer, J. Chem. Phys. **146**, 234503 (2017).
[47] J. Guo and J. C. Palmer, Phys. Chem. Chem. Phys. **20**, 25195 (2018).
[48] S. Plimpton, J. Comput. Phys. **117**, 1 (1995).
[49] S. Nösè, Mol. Phys. **52**, 255 (1984).
[50] W. G. Hoover, Phys. Rev. A **31**, 1695 (1985).
[51] B. Smit, J. Chem. Phys. **96**, 8639 (1992).
[52] D. Van Der Spoel, E. Lindahl, B. Hess, G. Groenhof, A. E. Mark, and H. J. C. Berendsen, J. Comput. Chem. **26**, 1701 (2005).
[53] U. Essmann, L. Perera, M. L. Berkowitz, T. Darden, H. Lee, and G. L. Pedersen, J. Chem. Phys. **103**, 8577 (1995).
[54] S. Miyamoto and P. A. Kollman, J. Comput. Chem. **13**, 952–962 (1992).
[55] C. Vega, J. L. F. Abascal, and I. Nezbeda, J. Chem. Phys. **125**, 034503 (2006).
[56] T. A. Kesselring, E. Lascaris, G. Franzese, S. V. Buldyrev, H. J. Herrmann, and H. E. Stanley, J. Chem. Phys. **138**, 244506 (2013).
[57] R. S. Singh, J. W. Biddle, P. G. Debenedetti, and M. A. Anisimov, J. Chem. Phys. **144**, 144504 (2016).
[58] J. W. Biddle, R. S. Singh, E. M. Sparano, F. Ricci, M. A. González, C. Valeriani, J. L. F. Abascal, P. G. Debenedetti, M. A. Anisimov, and F. Caupin, J. Chem. Phys. **146**, 034502 (2017).
[59] K. Binder, B. Block, S. K. Das, P. Virnau, and D. Winter, J. Stat. Phys. **144**, 690 (2011).
[60] K. Binder, B. J. Block, P. Virnau, and A. Tröster, Am. J. Phys. **80**, 1099 (2012).
[61] M. Fitzgerald, P. R. Picard, and R. N. Silver, Europhys. Lett. **46**, 282 (1999).
[62] J. R. Errington, Phys. Rev. E **67**, 012102 (2003).
[63] E. M. Grzelak and J. R. Errington, J. Chem. Phys. **128**, 014710 (2008).
[64] R. S. Singh, M. Santra, and B. Bagchi, J. Chem. Phys. **136**, 084701 (2012).
[65] P. J. Steinhardt, D. R. Nelson, and M. Ronchetti, Phys. Rev. B **28**, 784 (1983).
[66] P.-R. ten Wolde, M. J. Ruiz-Montero, and D. Frenkel, Faraday Discuss. **104**, 93 (1996).
[67] W. Lechner and C. Dellago, J. Chem. Phys. **129**, 114707 (2008).
[68] E. Shiratani and M. Sasai, J. Chem. Phys. **108**, 3264 (1998).
[69] A. Reinhardt, J. P. K. Doye, E. G. Noya, and C. Vega, J. Chem. Phys. **137**, 194504 (2012).
[70] A. Haji-Akbari and P. G. Debenedetti, Proc. Natl. Acad. Sci. U. S. A. **112**, 10582 (2015).
[71] J. C. Palmer, F. Martelli, Y. Liu, R. Car, A. Z. Panagiotopoulos, and P. G. Debenedetti, Nature **510**, 385 (2014).
[72] M. Matsumoto, S. Saito, and I. Ohmine, Nature **416**, 409 (2002).
[73] E. B. Moore and V. Molinero, Nature **479**, 506 (2011).
[74] R. S. Singh and B. Bagchi, J. Chem. Phys. **140**, 164503 (2014).
[75] M. Fitzner, G. C. Sosso, S. J. Cox, and A. Michaelides, Proc. Natl. Acad. Sci. U. S. A. **116**, 2009 (2019).
[76] J. C. Palmer, Proc. Natl. Acad. Sci. U. S. A. **116**, 1829 (2019).